THREE DIMENSIONAL SAR TOMOGRAPHY IN SHANGHAI USING HIGH RESOLUTION SPACE-BORNE SAR DATA

Lianhuan Wei, Timo Balz, Kang Liu, Mingsheng Liao

LIESMARS, Wuhan University, 129 Luoyu Road, 430079 Wuhan, China, lianhuan@whu.edu.cn

ABSTRACT

In this paper, we will demonstrate three-dimensional tomographic reconstruction of space-borne high-resolution SAR data using Shanghai as our test site. The high density of high-rise buildings in Shanghai leads to a rather complicated backscattering regime, which is difficult to handle with conventional interferometric processing. For the tomographic signal reconstruction, we use three different reconstruction methods: Singular Value Decomposition (SVD), Truncated SVD, and Wiener-SVD. We tested all three methods on simulated and real SAR data. In our experiments, we can demonstrate that SVD works only in a few cases. Truncated-SVD and Wiener-SVD deliver better results.

1. INTRODUCTION

With the new generation of Synthetic Aperture Radar (SAR) satellites, like for example TerraSAR-X and COSMO-SkyMed, data stacks with up to 0.6 meter resolution can be built up relatively fast. The surveillance of buildings in urban areas benefits from the high spatial resolution. Even details of building facades can be seen from space. However, with such a high resolution, the layover problem in dense urban areas gets obvious. Our previous research results show that in areas with many high buildings, it is difficult to interpret the result from standard PS-InSAR techniques. This is mainly due to the complicated backscattering scenarios and due to height estimation errors.

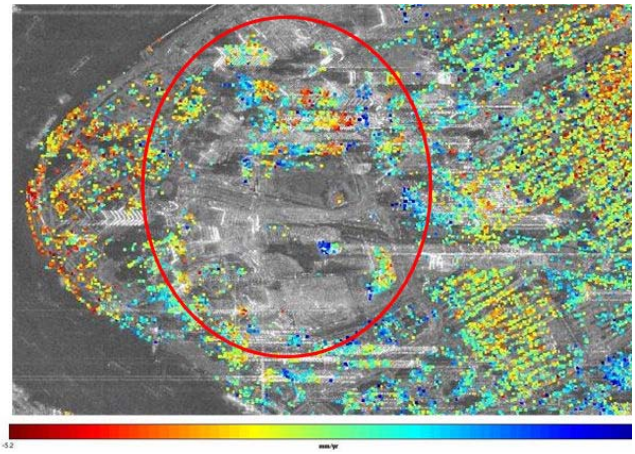

Figure 1. PS-InSAR results over Shanghai, Pudong area

Fig. 1 shows the PS-InSAR results using a stripmap TerraSAR-X image stack over Shanghai, which we will again use in section 3.2. The estimated deformation velocities and persistent scatterer heights are often wrong, mainly due to phase unwrapping errors at the very high buildings. This area with an extreme density of skyscrapers is not very suitable for InSAR processing. SAR images are 2D projection of the 3D scattering properties of the imaged terrain. As demonstrated with the example from Fig. 1, buildings and other vertical structures lead to massive layover ambiguities that are difficult to handle. SAR Tomography (TomoSAR) is a way of overcoming the limitations of the standard two-dimensional SAR imaging.

TomoSAR aims at retrieving the distribution of scatterers in elevation direction and their corresponding reflectivity from a stack of SAR acquisitions. Small orbit variations between the different acquisitions are used to form a synthetic aperture in elevation direction, the so-called elevation aperture. By spectral estimation, with special consideration of the difficulties caused by sparse and irregular sampling, a reflectivity profile is retrieved for each azimuth-range pixel. The reflectivity profile is used to estimate scattering parameters, such as the number of scatterers in a pixel, their elevations, and their reflectivity strength.

The idea of tomographic imaging in radar was proposed by Farhat *et al.* [1] and introduced to SAR in 1994 by Piau [2]. The first experiments in TomoSAR were carried out in a laboratory under ideal experimental conditions [3] and using airborne systems [4]. In 2005, Fornaro *et al.* retrieved the scattering profile of a stadium in Naples, Italy, from C-band ERS data [5]. In 2006, Fornaro & Serafino separated the single- and double-scatterer cases [6].

Lombardini [7] extended the SAR tomography into Differential TomoSAR by taking the long-term motion of objects into account. Recently Zhu & Bamler [8] demonstrated the reconstruction of non-linear, seasonal motion with D-TomoSAR. Also Fornaro *et al.* [9] showed the 5D reconstruction (space-velocity-dilation) with TomoSAR.

In the following section, we will describe our methodology. In section 3, we show the results of our experiments with simulated and real SAR data. Finally, conclusions are drawn.

Proc. 'Fringe 2011 Workshop', Frascati, Italy,
19–23 September 2011 (ESA SP-697, January 2012)

2. METHODOLOGIES

2.1TomoSAR System Model

A SAR image is referenced to the azimuth-slant range plane. The third direction, which is perpendicular to the azimuth-slant range plane, is called elevation direction. The 3D reference frame is represented as (x, r, s), with x representing the azimuth direction, r representing the range direction, and s representing the elevation. The complex value of each pixel in a focused complex SAR image presents a projection along the elevation direction of the illuminated 3D backscattering properties over the azimuth-slant range plane [10]. SAR tomography (TomoSAR) retrieves the distribution of scatterers in the elevation direction and the corresponding reflectivity from a stack of N complex SAR datasets of the same area taken at slightly different orbit positions.

$$g_n = \int_{\Delta s} \gamma(s) exp(-j2\pi\xi_n s) ds \quad (1)$$

where $(n = 1, \dots, N)$. N is the number of SAR images, $\gamma(s)$ represents the reflectivity function along s, Δs is the extent of signal along s, and $\xi_n = -2b_n/(\lambda r)$ is the spatial elevation frequency. The continuous imaging model could be approximated and discretized along s within its extent Δs, in the presence of noise ε, and can be written as:

$$g = R\gamma + \varepsilon \quad (2)$$

where $g = (g_1, g_2, \dots, g_N)^T$ is the measurements vector with N elements. R is a $N \times L$ mapping matrix with $R_{nl} = exp(-j2\pi\xi_n s_l)$. γ is the discrete reflectivity vector with L elements, $\gamma_l = \gamma(s_l)$, and $s_l (l = 1, \dots, L)$ are the discrete elevation positions.

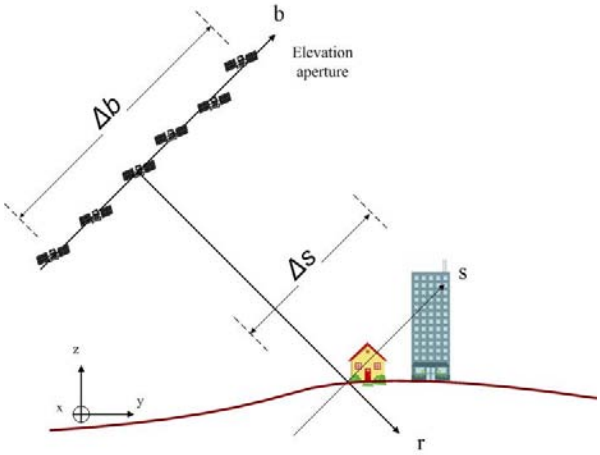

Figure 2.TomoSAR principle

In Fig. 2 the basic geometry of TomoSAR is shown. In TomoSAR, a data stack of several acquisitions from slightly different viewing angles is used to reconstruct the reflectivity function along the elevation direction. The combination of these several acquisitions is used to form the so-called elevation aperture. Using spectral analysis for every azimuth–range pixel a focused 3D SAR image is obtained [11]. The objective of TomoSAR is to retrieve the reflectivity profile for each azimuth–range pixel and then use it to estimate scattering parameters such as the number of scatterers present in the cell, their elevations, and reflectivities. It is essentially a spectral estimation problem.

For non-parametric spectral analysis, the expected elevation resolution ρ_s, *i.e.* the width of the elevation point response function, depends on the elevation aperture size Δb, and is approximately:

$$\rho_s = \frac{\lambda r}{2\Delta b} \quad (3)$$

where r is the distance between SAR acquisition center and the sensor.

2.2 Singular Value Decomposition

The singular value decomposition (SVD) is widely used in signal processing and statistics. It is a simple and valuable tool for analyzing image quality and the amount of independent information about the unknowns in presence of noise.

Let $G \in R^{m \times n}$ be a rectangular matrix with $m > n$. The SVD of G is a decomposition of the form [12]:

$$G = U \sum V^T = \sum_{i=1}^{n} u_i \sigma_i v_i^T \quad (4)$$

where $U = (u_1, \dots, u_n)$ and $V = (v_1, \dots, v_n)$ are matrices with orthonormal columns, $U^T U = V^T V = I_n$ and $\sum = diag(\sigma_1, \dots, \sigma_n)$ has non-negative diagonal elements such that $\sigma_1 \geq \cdots \geq \sigma_n \geq 0$. σ_i are the singular values of G while the vectors u_i and v_i are the left and right singular vectors of G respectively. The discrete reflectivity signal γ can be reconstructed from measurement g through pseudo inversion of R,

$$\hat{\gamma} = R^* g = \sum_{n=1}^{N} \sigma_n^{-1} (u_n^T g) v_n \quad (5)$$

However, noise propagation caused by small singular values may lead to wrong reconstruction results and regularization tools are required.

Truncated SVD (TSVD) [13] is a well-known method to deal with an ill-conditioned matrix. The basic idea of TSVD and other regularization tools is to impose additional requirements on the solution and look for an approximate reliable solution. TSVD truncates small singular values by setting a threshold according to the noise level.

Another regularization tool used in this work is Wiener filtering [14]. Wiener filtering gives weights to the singular values according to their magnitude, which avoids choosing a hard threshold.

We tested all three methods with simulated data and with TerraSAR-X stripmap data over Shanghai.

3. EXPERIMENTS

3.1 Simulated Results

Based on typical TerraSAR-X orbit histories, a real baseline of TerraSAR-X Spotlight data is used for the simulation. We use system parameters comparable to those of the TerraSAR-X satellite mission as shown in Tab. 1. The baseline distribution and corresponding singular values are shown in Fig. 3. The baseline range is about 368m, which results in a 29.7m resolution in elevation direction.

Table1. Initialization parameters of the simulated signal

Distance from scene center	R	704000m
Wavelength	λ	0.031m
Actual number of acquisitions	N	20

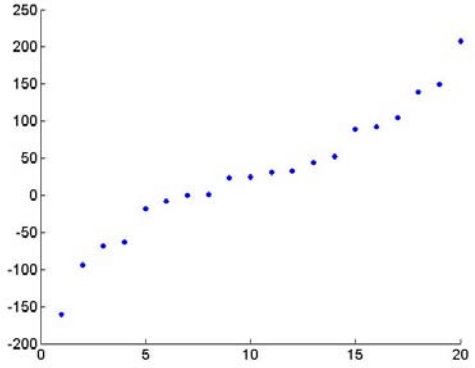

(a) Baseline Distribution

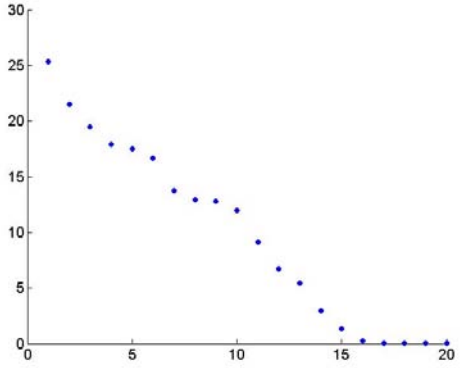

(b) Singular Values

Figure 3. The baseline distribution of the simulated dataset and their singular values

Two scatterers with the same reflectivity power located at -30m and 30m along elevation direction are simulated. The reconstructed reflectivity profiles from SVD, TSVD, and Wiener-SVD are shown in Fig. 4. SVD without any regularization methods present the worst result, which is caused by noise propagation due to small singular values. Both TSVD and Wiener-SVD show better performances.

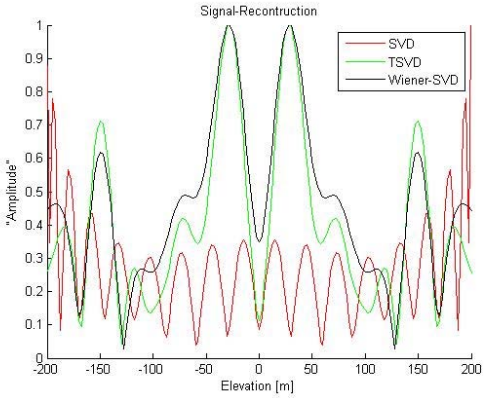

Figure 4. Reconstructed reflectivity profile from SVD, TSVD, and Wiener-SVD

3.2 Real Data Processing

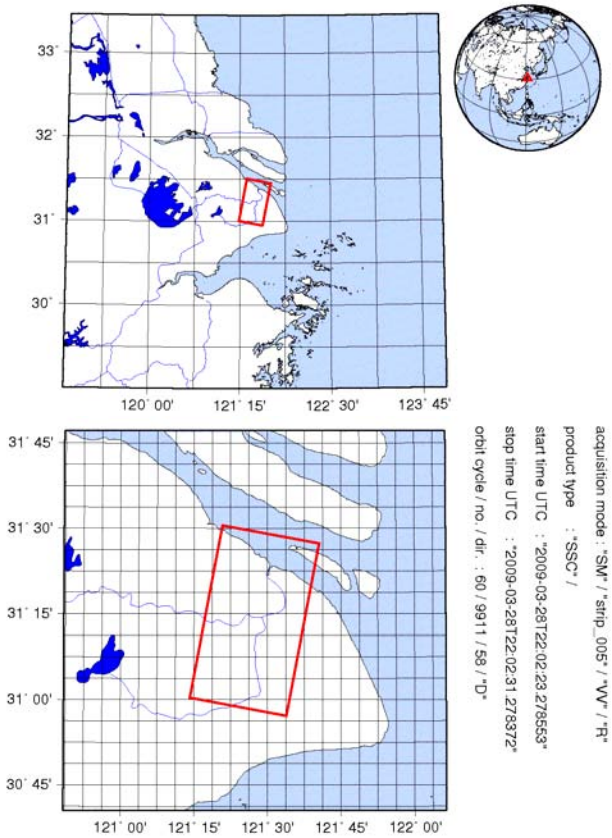

Figure 5. The TerraSAR-X scene coverage

We selected the Shanghai Stadium as test area for our experiments. The stack used for our experiments consists of 20 TerraSAR-X stripmap images acquired from April 2008 to January 2010 with a baseline range of 361.36 m and a target distance of 566.3 km.

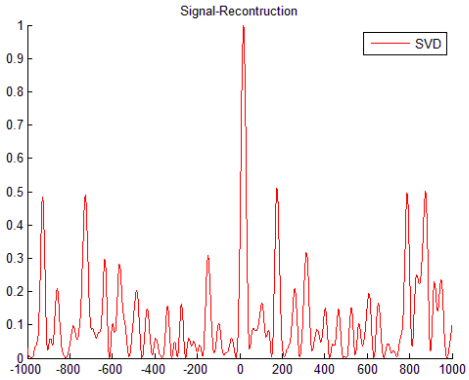

(a)

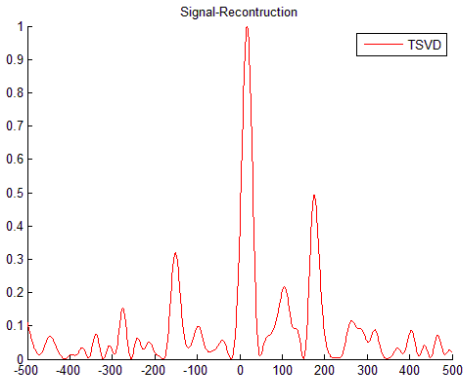

(b)

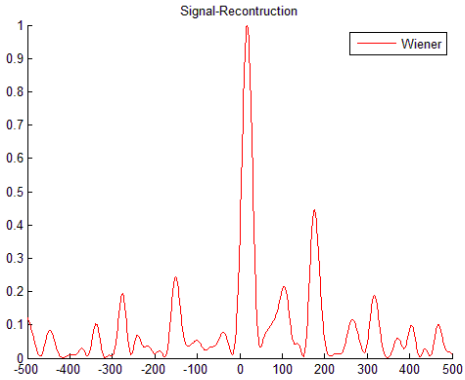

(c)

Figure 6. Signal reconstruction in elevation using SVD (a), TSVD (b), and Wiener-SVD (c)

The approximated resolution in elevation is 24.4m. We did not estimate the atmospheric phase screen, but use a stable reference point for processing the data. Based on the amplitude stability we select a reference point *R* on the ground (see Fig. 8) and the test point *P1* nearby.
As can be seen in Fig. 6, the single reflection center can be reconstructed using SVD, TSVD, and Wiener-SVD. Using SVD a larger elevation size has to be reconstructed (from -1000 to 1000m) compared to TSVD and Wiener-SVD, which are being reconstructed from -500 to 500m.

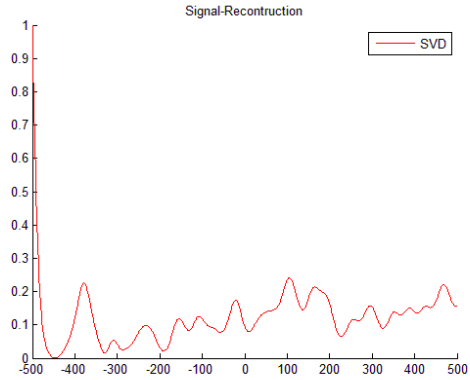

(a)

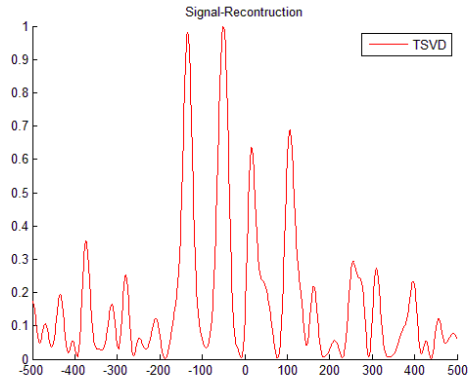

(b)

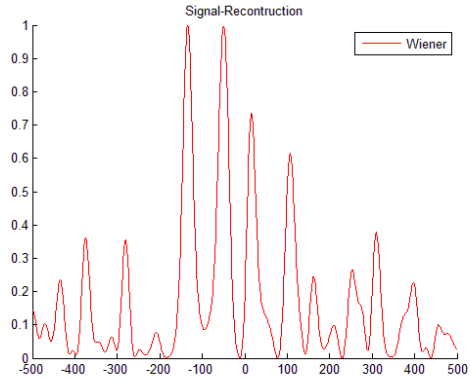

(c)

Figure 7. Signal reconstruction in elevation from a point containing two reflection centers using SVD (a), TSVD (b), and Wiener-SVD (c)

As second test point *P2* we select a point on top of the stadium. The point is stable and has two contributions: one from the stadium and a second one from a tower behind the stadium (see Fig. 9). The height difference between the points is estimated to be around 45 m, which is approximately 90 m in elevation direction.
As shown in Fig. 7, no signal can be reconstructed using SVD, but with TSVD and Wiener, two signal peaks can be clearly reconstructed. The distance in elevation is 85 m, which fits pretty well to our assumptions.

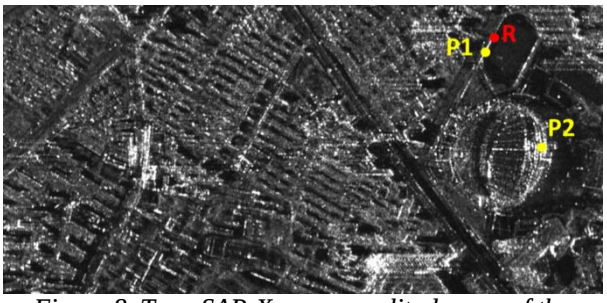

Figure 8. TerraSAR-X mean amplitude map of the Shanghai stadium test area with the reference point R and the test points P1 and P2.

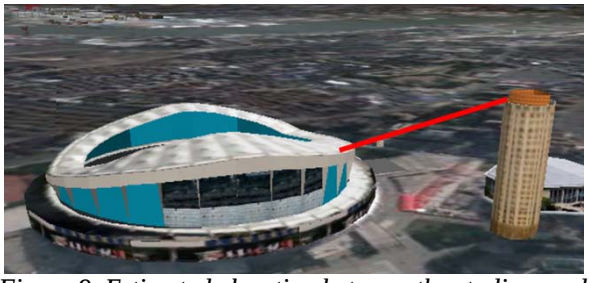

Figure 9. Estimated elevation between the stadium and the tower in far range of the stadium

4. CONCLUSION

3D Tomographic results from both simulated data and TerraSAR-X data are presented in this work. The 3D reflectivity reconstruction capability and the multi-scatterers separation capability of SAR tomography are demonstrated. We showed that TSVD and Wiener SVD, work well on simulated and real data. SVD alone only works in a few test cases. In the future, we will extend the 3D SAR tomography into 4D SAR tomography.

ACKNOWLEDGMENT

This work is supported by the International Graduate School of Science and Engineering, Technische Universität München, Munich, Germany, by the National Key Basic Research and Development Program of China under Grant 2007CB714405, and by "the Fundamental Research Funds for the Central Universities" in China, Project No. 904274488. The authors would also like to thank the Infoterra GmbH and Beijing Spot image for providing the test datasets.

REFERENCES

1.Farhat, N., Werner, C. & Chu, T. (1984). Prospects for three-dimensional projective and tomographic imaging radar networks. *Radio Science.***19** (5), 1347–1355.

2.Piau, P. (1994). Performances of the 3D-SAR imagery. In *Proceedings of IEEE International Geoscience and Remote Sensing Symposium (IGARSS)*, Vol.4, pp. 2267–2271.

3.Pasquali, P., Prati, C., Rocca, F., Seymour, M., Fortuny, J., Ohlmer, E., & Sieber, A. (1995). A3-D SAR experiment with EMSL data. In *Proceedings of IEEE International Geoscience and Remote Sensing Symposium (IGARSS)*, Vol. 1, pp. 784–786.

4.Reigber, A. & Moreira, A. (2000) First demonstration of airborne SAR tomography using multibaseline L-band data. *IEEE Transactions on Geoscience and RemoteSensing***38**, 2142–2152.

5.Fornaro, G. ,Lombardini, F. & Serafino, F. (2005). Three-dimensional multipass SAR focusing: Experiments with long-term spaceborne data. *IEEE Transactions on Geoscience and RemoteSensing***43** (4), 702–714.

6.Fornaro, G. & Serafino, F. (2006). Imaging of Single and Double Scatterers in Urban Areas via SAR Tomography. *IEEE Transactions on Geoscience and Remote Sensing***44** (12), 3497–3505.

7. Lombardini, F. (2005). Differential tomography: a new framework for SAR interferometry. *IEEE Transactions on Geoscience and Remote Sensing***43** (1), 37-44.

8. Zhu, X. &Bamler, R. (2011). Let's Do the Time Warp: Multicomponent Nonlinear Motion Estimation in Differential SAR Tomography. *IEEE Geoscience and Remote Sensing Letters***8**(4), 735-739.

9. Fornaro, G., Pauciullo, A., Reale, D., Zhu, X. & Bamler, R. (2011). Peculiarities of urban area analysis with very high resolution interferometric SAR data. In Proc. *JURSE 2011 - Joint Urban Remote Sensing Event*, Munich, Germany, pp. 185-188.

10.Fornaro, G., Serafino, F. & Soldovieri, F. (2003). Three-dimensional focusing with multipass SAR data. *IEEE Transactions on Geoscience and Remote Sensing* **41** (3), 507–517.

11.Zhu, X. & Bamler, R. (2010). Very High Resolution Spaceborne SAR Tomography in Urban Environment. *IEEE Transactions on Geoscience and Remote Sensing* **48** (12), 4296–4308.

12.Hansen, P. (1994). Regularization tools: A Matlab package for analysis and solution of discrete ill-posed problems. *Numerical Algorithms***6** (1), 1–35.

13.Hansen, P. (1987). The truncated SVD as a method for regularization. *BIT Numerical Mathematics***27** (4), 534–553.

14. Zhu, X. (2008). High-Resolution Spaceborne Radar Tomography. Technische Universität München, Master's thesis, Munich, Germany.